



## LABORATORY Spotlight

The National High Magnetic Field Laboratory

Reprinted from NHMFL Reports Fall 2001

National High Magnetic Field Laboratory • 1800 East Paul Dirac Drive, Tallahassee, Florida 32310 • 850 644-0311 • <http://www.magnet.fsu.edu>

# High Capacity Production of > 40% Spin Polarized Xenon-129 for NMR and MRI Applications at the NHMFL

Anthony L. Zook and Clifford R. Bowers, UF, Chemistry

**T**he NHMFL and the University of Florida recently supported the development of a hyperpolarized noble gas generator at UF. We are pleased to report that construction of this facility is now complete, and that its performance for high capacity hyperpolarized  $^{129}\text{Xe}$  production is apparently better than any other laser diode array (LDA) based system reported in the literature. Here, we show the results of the performance tests, and to demonstrate the capability that is now available, several images obtained using the new polarizer will be presented. It is hoped that these promising results will stimulate interest in hyperpolarized noble gas applications that may now be pursued at the NHMFL.

Non-equilibrium methods for enhancing the nuclear spin polarization, and hence the signal-to-noise ratio in NMR experiments, are making a significant impact in certain types of NMR and MRI applications. These enhancement techniques include: dynamic nuclear polarization,<sup>1,2</sup> parahydrogen induced nuclear polarization,<sup>3,4</sup> optical pumping in solids,<sup>5,6,7</sup> and spin-exchange optical pumping of  $^{129}\text{Xe}$  and  $^3\text{He}$ .<sup>8,9</sup> Spin-exchange optical pumping, proven to be one of the more generally applicable methods, involves polarization of the hyperfine sublevels by repeated optical excitation of an alkali metal atom with circularly polarized light. Spin angular momentum exchange collisions between the alkali atom and  $^3\text{He}$  or  $^{129}\text{Xe}$  leads to the accumulation of a large nonequilibrium nuclear polarization, referred to as *hyperpolarization*, of the noble gas. While spin exchange optical pumping at low magnetic field had been known since the 1960's, it was not until the demonstration of Raftery *et al.*<sup>9</sup> that the hyperpolarized noble gas can be separated from the alkali metal and employed in enhanced sensitivity

high field NMR. This led Albert and co-workers<sup>10</sup> to demonstrate that hyperpolarized  $^{129}\text{Xe}$  could be used to obtain *in vivo* magnetic resonance images. Later,  $^3\text{He}$  was applied to the imaging of human lungs,<sup>11</sup> and now the technology of spin exchange optical pumping has even been commercialized<sup>12</sup> due to its excellent potential as a clinical diagnostic. In recent years, the number of spectroscopic applications of hyperpolarized  $^{129}\text{Xe}$  has also grown rapidly.

The key parameters affecting the maximum attainable nuclear polarization of  $^{129}\text{Xe}$  include the Rb vapor density (directly related to the pumping cell temperature), the pumping gas composition and pressure, the laser linewidth, and the laser power.<sup>13</sup> The parameters affecting the maximum attainable nuclear polarization of  $^{129}\text{Xe}$  include the Rb vapor density (directly related to the pumping cell temperature), the pumping gas composition ( $\text{Xe}$ ,  $\text{N}_2$ , and  $^4\text{He}$ ), the pumping time or flow rate, the pumping cell wall coating, the pumping field, and the laser linewidth and power.<sup>13</sup> Two types of near infrared laser systems are currently in common use for Rb-Xe spin exchange optical pumping: the titanium sapphire laser and the LDA. While the power available from the titanium sapphire ring laser is typically only a few watts, the laser line width is much narrower than the Doppler linewidth. The laser power is, therefore, efficiently absorbed by a suitably dense Rb vapor, and for this reason, the titanium sapphire laser is well suited to the production of small quantities (c.a.  $10\text{ cm}^3$ ) of >50% polarized  $^{129}\text{Xe}$  at pressures up to about 10 to 50 mbar.<sup>14</sup> With the advent of the LDA, much higher optical power tunable to the Rb  $^1\text{D}$  absorption line at a wavelength of 794.8 nm is available, but the linewidth of the output is typically on the order of 1000 GHz, a value greatly exceeding the  $\approx 1\text{ GHz}$  Doppler broadening of atomic Rb (at  $\approx 100^\circ\text{C}$ ). For spin exchange optical pumping of  $^{129}\text{Xe}$ , studies

have shown that a 98%  $^4\text{He}$ , 1%  $\text{N}_2$ , and 1%  $^{129}\text{Xe}$  gas composition provides the necessary pressure broadening for efficient optical absorption, reduction of spin-rotation relaxation of the  $^{129}\text{Xe}$ , and quenching of the alkali-atom excited state to reduce depolarization due to radiation trapping.<sup>13</sup> With the greater optical power available with LDAs, much higher alkali metal atom densities can be excited, and the rate of nuclear polarization of the  $^{129}\text{Xe}$  gas is proportionally greater due to the increased rate of Xe-Rb spin exchange collisions. The higher rate of polarization enables a flow mode of operation whereby the Xe/ $\text{N}_2$ /He gas mixture passes through the cell continuously. The LDA-based polarized gas generator is, therefore, advantageous in applications requiring large quantities of polarized gas such as magnetic resonance imaging,<sup>15</sup> enhanced NMR spectroscopy using hyperpolarized liquid  $^{129}\text{Xe}$ ,<sup>16,19</sup> and phase-cycled or two-dimensional NMR experiments.

**Table 1.** Survey of  $^{129}\text{Xe}$  polarizer data reported in the literature.

Research Group	Institution	LDA Power (W)	P, %	Xe Flow (sccm)	Production Factor*	Ref.
Appelt	Research Centre Jülich, Germany	50	20	2@26%	40	17
Chupp	U. Michigan	30	3.5	-	-	18
Conradi/Saam	Washington U.	40	5	2.4@26%	12	19
Happer	Princeton U.	50	5	6@71%	30	20
		100	18	3.2@71%	57.2	16
MITI	U. Virginia (15)	120	7	16.6@26%	117	21
	Duke (14)	120	10	12.2 @82%	122	22
	Duram, N.C. (4)	100	21	3	63	12
Pietrass	New Mexico Tech	45	1.5	37@26%	55.5	23
Pines	UC Berkeley	100	10	3@26%	30	24
Raifery	Purdue	100	4.5	2@26%	9	25
Ripmeester	NRC, Canada	30	6	2@26%	12	26
Segebarth	Université Joseph Fourier, France	150	8	16@26%	128	27
Walsworth	Harvard U.	15	5	-	-	15

Table 1 presents a survey of the  $^{129}\text{Xe}$  optical pumping systems described in the recent literature according to LDA power,  $^{129}\text{Xe}$  nuclear spin polarization produced, and Xe flow rate. Two relevant criteria by which the performance of a polarized gas generator can be evaluated are the maximum polarization achieved and the nuclear magnetization production rate, a quantity proportional to the product of the nuclear polarization and the Xe flow rate. There is a wide variation in the reported values of the nuclear polarization (or signal enhancement factor) and production factor, but in summary, the polarization achieved in previous LDA systems is substantially lower than the value achieved in titanium sapphire systems.

Ideally, a hyperpolarized noble gas generator would simultaneously deliver both high capacity and the highest possible polarization. Previous work suggests that higher polarization and high flow rates may potentially be obtained by increasing the rubidium density and absorbed laser power.<sup>17</sup> However, an experimental investigation to determine if this is so requires a higher power LDA system than has been previously available. The NHFML-UF polarized gas generator employs a 210 W LDA, to our knowledge, the highest optical power yet to be employed in  $^{129}\text{Xe}$  spin exchange optical pumping.

A schematic of the NHMFL-UF polarizer is shown in Fig. 1. The laser system consists of seven fiber coupled LDA units, each with an output of 30 W at 795 nm, and with a total combined line width of 1.7 nm (~800 GHz). The individual fiber outputs are combined into a single fiber terminated by a water-cooled output connector. The individual fibers are embedded in a high-thermal conductivity epoxy and are anti-reflection coated to minimize heating at the connector. The unpolarized beam emerging from the optical fiber passes through a collimating lens and then is split into horizontally and linearly polarized beams by a beam-splitting cube. The two beams are circularly polarized with the same sense of helicity by two separate quarter-wave plates and superimposed at a distance of 80 cm using an adjustable mirror mount. This optical polarizer arrangement permits the full power of the laser system to be circularly polarized even though the output of the LDA system is unpolarized.

The 5x12 cm cylindrical optical pumping cell has an inlet and outlet to facilitate continuous flow generation of hyperpolarized  $^{129}\text{Xe}$ . PFA tubing with non-magnetic fittings connects the pumping cell to the NMR probe. After passing through the probe, the gas can either be vented (in applications where it may become contaminated) or recirculated by a magnetically coupled pump. The flow rate is monitored and adjusted by a needle valve on the return line.

As noted above, the rate of optical pumping of the rubidium vapor depends on the fraction of the laser

power absorbed by the vapor. The main parameters affecting the absorption are (1) the buffer gas pressure and (2) the rubidium density that is determined by the optical pumping cell “conditioning” and the temperature. To obtain optimal absorption a fiber coupled CCD optical spectrometer monitors

in an LDA-based polarizer, and furthermore, the rate of magnetization production is also higher than any other literature report at any flow rate. These performance characteristics are attributed to the high laser power, narrow laser line width, and efficient polarizer design.

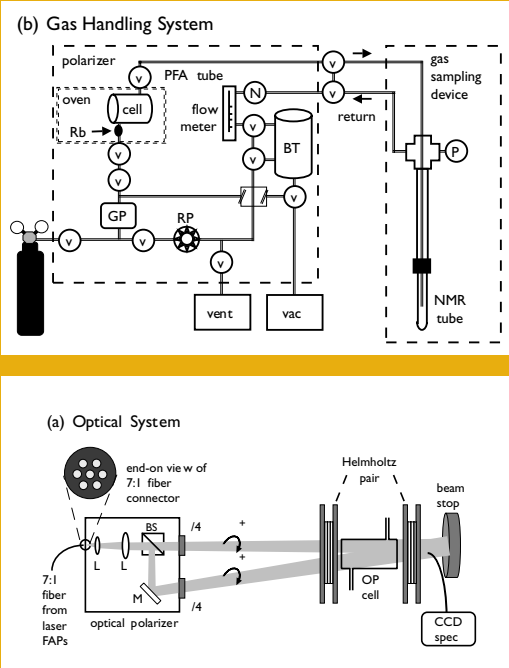


**Figure 1.** (a) Optical System. BS=beam splitter, L=lens, and M=mirror. (b) Gas handling system. RP=recirculation pump, GP=gas purifier, P=pressure gauge, BT=ballast tank, v=valve, and N=needle valve.

the transmission of the laser light through the pumping cell. For example, Fig. 2a presents the optical transmission as a function of the pumping cell temperature at a gas pressure of 3400 Torr. At 100 °C, the Rb density is too low and the light is not absorbed, while at 170 °C the density is too high, and in this case the pumping light does not reach the back of the cell. The intermediate temperature of 140 °C represents the optimal situation where the Rb will be maximally polarized over the entire pumping cell volume.

The performance characteristics of the UF/NHMFL hyperpolarized noble gas generator are presented in Table 2. The highest  $^{129}\text{Xe}$  polarization obtained from this system was 46.2% in batch mode and 40.% in continuous flow mode.<sup>28</sup> It appears that these are the highest levels of polarization to be achieved

Finally, Fig. 3 demonstrates the capability of performing magnetic resonance imaging experiments on  $^{129}\text{Xe}$  gas and  $^{129}\text{Xe}$  liquid using the UF/NHMFL hyperpolarized gas generator. In each case, a cross section of the cylindrical NMR tube was imaged with a 10 mm high resolution probe using a small pulse angle gradient echo filtered imaging (GEFI) pulse sequence. To obtain the  $^{129}\text{Xe}$  liquid image, the hyperpolarized gas was first condensed as a solid at a temperature several degrees below the melting point. The image was obtained after raising the probe temperature to form liquid Xe in the sample tube. In principle, magnetic resonance imaging with liquid Xe at this level of polarization should yield higher resolution than proton imaging of liquid water.

In summary, the laser-polarized noble gas generator incorporating a 210 W laser diode array has been constructed and tested, and a nuclear polarization of 46.2% of  $^{129}\text{Xe}$  has been obtained. The  $^{129}\text{Xe}$  nuclear polarization obtained with this new system easily competes with Ti:sapphire based polarizers, but the capacity of the UF/NHMFL LDA system, in terms of the rate of  $^{129}\text{Xe}$  magnetization produced, is far

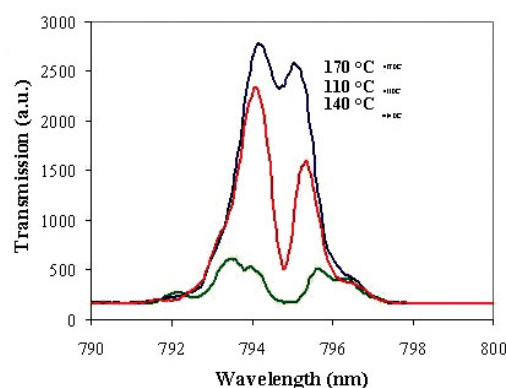


**Figure 2.** Optical transmission of pumping cell as a function of cell temperature.

**Table 2.** UF/NHMFL polarizer characteristics.

Laser Power (W)	P, %	Xe:N <sub>2</sub> :He Composition	Xe Flow Rate (sccm)	Production Factor
210	40	1:1:98	4.8@86%	192
210	23	2:2:96	7.44@26%	171
210	12	5:5:90	18.6@26%	223

greater. The ability to produce highly polarized  $^{129}\text{Xe}$  at rates in excess of 1 liter-atm/hour will facilitate superior results in 1D and 2D NMR as well as MRI applications. Since the NMR signal obtained from liquid  $^{129}\text{Xe}$  polarized to  $> 40\%$  exceeds the proton signal of liquid  $\text{H}_2\text{O}$ , improved resolution in imaging applications should be possible. Potential spectroscopic applications include protein studies, surface NMR, and polarization transfer enhancement on surfaces. In conclusion, we hope that the promising initial results obtained with the NHMFL-UF polarizer will stimulate researchers of the NHMFL in-house and user community to consider experiments using this new instrument. Potential users should contact Russ Bowers, Steve Blackband, Anthony Brennan, or Steve Gibbs.

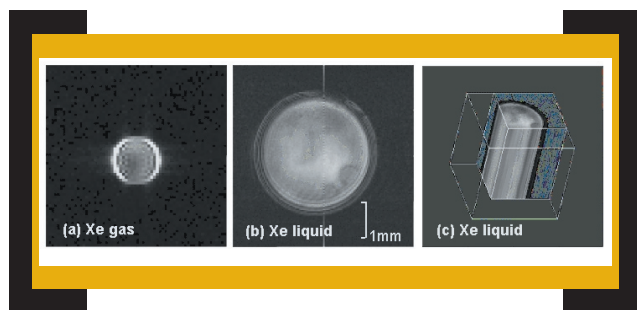


**Figure 3.** (a) Axial non-slice-selective gradient echo image of polarized xenon gas flow. The increased intensity near the walls of tubing is indicative of wall restricted diffusion of the gas. (b) Single scan gradient echo image of polarized liquid xenon at 186 K. Total experiment time was 20 seconds. Outer ringing of image was caused by clipping of the FID during acquisition. (c) 3D single scan, multiple gradient echo image (5 slices) of polarized liquid xenon in a cylindrical sample cell at 186 K, acquired with a tip angle  $4^\circ$ . The total experiment time was 20 seconds.

**Acknowledgements:** The authors gratefully acknowledge receiving advice and assistance from Stephen Blackband, Sam Grant, and Pete Thelwall. Anthony Zook was supported as a graduate research assistant by NIH resource grant P41 RR16105 (S. Blackband, PI). Funding for this project was provided by the University of Florida and the NHMFL In-House Research Program (C. Bowers, S. Blackband, A. Brennan, S. Gibbs, and S. Smith).

- <sup>1</sup> Abragam, A., and Goldman, M., *Nuclear Magnetism, Order and Disorder* (Clarendon, Oxford); Bowers, C.R. and Weitekamp, D.P., *J. Am. Chem. Soc.*, **109**, 5541 (1987).
- <sup>2</sup> Farrar, C.T., Hall, D.A., Gerfen, G.J., Inati, S.J., and Griffin, R.G., *Mechanism of Dynamic Nuclear Polarization in High Magnetic Fields*, *J. Chem. Phys.* **114**, 4922-4933 (2001).
- <sup>3</sup> Bowers, C.R. and Weitekamp, D.P., *Phys. Rev. Lett.*, **57**, 2645 (1986); Bowers, C.R., Weitekamp, D.P., *J. Am. Chem. Soc.* **109**, 5541 (1987).
- <sup>4</sup> Duckett, S.B., and Sleight, C.J., *Prog. Nucl. Magn. Reson. Spectrosc.*, **34**, 71 (1999).
- <sup>5</sup> Ekimov, A.I., and Safarov, V.I., *JETP Lett.*, **15**, 179 (1972).
- <sup>6</sup> Barrett, S.E., Tycko, R., Pfeiffer, L.N. and West, K.W., *Phys. Rev. Lett.*, **72**, 1368 (1994).
- <sup>7</sup> Bowers, C.R., *Solid State NMR*, **11**, 11 (1998).
- <sup>8</sup> Happer, W., *Rev. Mod. Phys.*, **44**, 169 (1972).
- <sup>9</sup> Raftery, D., Long H., Meersman, T., Grandinetti, P.J., Reven, L., and Pines, A., *Phys. Rev. Lett.*, **66**, 584 (1991).
- <sup>10</sup> Albert, M.S., *et al.*, *Nature* (London) **370**, 199 (1994).
- <sup>11</sup> MacFall, J.R., *et al.*, *Radiology*, **200**, 553 (1996).
- <sup>12</sup> Magnetic Imaging Technologies, Inc., 2500 Meridian Parkway, Suite 175, Durham, NC 27713.
- <sup>13</sup> Driehuys, B., Cates, G., Miron, E., Sauer, K., Walter, K., and Happer, W., *Appl. Phys. Lett.*, **69**, 1668 (1996).
- <sup>14</sup> Ruth, U., Hof, T., Schmidt, J., Fick, D., and Jansch, H.J., *Appl. Phys. B*, **68**, 93 (1999).
- <sup>15</sup> Tseng, C.H., Mair, R.W., Wong, G.P., Williamson, D., Cory, D.G., and Walsworth, R.L., *Phys. Rev. E*, **59**, 1785 (2001).
- <sup>16</sup> Fitzgerald, R.G., Sauer, K.L., and Happer, W., *Chem. Phys. Lett.*, **284**, 87 (1998).
- <sup>17</sup> Shah, N., Timur, U., Wegener, H., Halling, H., Zilles, K., and Appelt, S., *NMR Biomed.*, **13**, 214 (2000).
- <sup>18</sup> Welsh, R.C., Chupp, T.E., Coulter, K.P., Rosen, M.S., Swanson, S.D., and Agranoff, B.W., *Nucl. Instr. and Meth. A*, **402**, 461 (1998).
- <sup>19</sup> Leawoods, J., Saam, B., and Conradi, M., *Chem. Phys. Lett.*, **327**, 359 (2000).
- <sup>20</sup> Driehuys, B., Cates, G., Miron, E., Sauer, K., Walter, K., and Happer, W., *Appl. Phys. Lett.*, **69**, 1668 (1996).
- <sup>21</sup> Ruppert, K., Brookman, J.R., Hagspiel, K.D., Driehuys, B., and Mugler, J.P., III, *NMR Biomed.*, **13**, 220 (2000).
- <sup>22</sup> Chen, X.J., *et al.*, *Mag. Res. Med.*, **42**, 721 (1999).
- <sup>23</sup> Kneller, J., Soto, R., Surber, S., Colomer, J., Fonseca, A., Nagy, J., Pietrass, T., *J. Mag. Reson.*, **147**, 261 (2000).
- <sup>24</sup> Meersmann, T., Logan, J., Simonutti, R., Caldarelli, S., Comotti, A., Sozzani, P., Kaiser, L., and Pines, A., *J. Phys. Chem. A*, **104**, 11665 (2000).
- <sup>25</sup> Smith, L., Smith, J., MacNamara, E., Knagge, K., Raftery, D., *J. Phys. Chem. B*, **105**, 1412 (2001).
- <sup>26</sup> Moudrakovski, L., Lang, S., Ratcliffe, C., Simard, B., Santyr, G., and Ripmeester, J., *J. Mag. Res.*, **144**, 372 (2000).
- <sup>27</sup> Duhamel, G., unpublished results.
- <sup>28</sup> Zook, A.L. and Bowers, C.R., *submitted for publication*.